INTECH
open science | open minds

OPEN ACCESS
ARTICLE

International Journal of Advanced Robotic Systems

Intelligent Navigation for a Solar Powered Unmanned Underwater Vehicle

Regular Paper

Francisco García-Córdova[1] and Antonio Guerrero-González[1,*]

1 Department of Systems Engineering and Automation, Universidad Politécnica de Cartagena (UPCT), Cartagena-Murcia, Spain
* Corresponding author E-mail: antonio.guerrero@upct.es

Received 31 May 2012; Accepted 31 Jan 2013

DOI: 10.5772/56029

Abstract In this paper, an intelligent navigation system for an unmanned underwater vehicle powered by renewable energy and designed for shadow water inspection in missions of a long duration is proposed. The system is composed of an underwater vehicle, which tows a surface vehicle. The surface vehicle is a small boat with photovoltaic panels, a methanol fuel cell and communication equipment, which provides energy and communication to the underwater vehicle. The underwater vehicle has sensors to monitor the underwater environment such as sidescan sonar and a video camera in a flexible configuration and sensors to measure the physical and chemical parameters of water quality on predefined paths for long distances. The underwater vehicle implements a biologically inspired neural architecture for autonomous intelligent navigation. Navigation is carried out by integrating a kinematic adaptive neuro-controller for trajectory tracking and an obstacle avoidance adaptive neuro- controller. The autonomous underwater vehicle is capable of operating during long periods of observation and monitoring. This autonomous vehicle is a good tool for observing large areas of sea, since it operates for long periods of time due to the contribution of renewable energy. It correlates all sensor data for time and geodetic position. This vehicle has been used for monitoring the Mar Menor lagoon.

Keywords Underwater Vehicles, Behaviour-Based Control, Neural Network, Solar Unmanned Underwater Vehicles

1. Introduction

1.1 Autonomous Underwater Vehicles

The need for autonomous underwater robots has become increasingly apparent as the world pays greater attention to environmental and resource issues as well as scientific and military tasks. Many autonomous underwater robots have been developed to overcome scientific challenges and the engineering problems caused by the unstructured and hazardous underwater environment.

With continuous advances in control, navigation, artificial intelligence, material science, computers, sensors and communication, autonomous underwater vehicles (AUVs) have become very attractive for various underwater tasks. Autonomy is one of the most critical issues in developing AUVs. The design, development, navigation and control process of an AUV is a complex and expensive task. Various control architectures have been studied to help increase the autonomy of AUVs [1-9].

There is a large amount of research underway to investigate enabling technologies to allow further development of autonomous underwater robot systems. Control of AUVs in uncertain and non-structured environments is a complex process involving nonlinear dynamic behaviour. Various advanced underwater robot control systems have been proposed, such as sliding mode control (SMC) by Yoerger and Slotine in 1984 [3], nonlinear control by Nakamura and Savant in 1992 [4], adaptive control by Antonelli et al. in 2001 [5], neural network control by Lorenz and Yuh in 1996 [6] and Porto and Fogel in 1992 [7], fuzzy control by Smith et al. [8] and visual servo control by Silpa-Anan et al. in 2001 [9].

1.2 Solar Powered Underwater Vehicle

The need for different data collection in situ, on different scales in time and space, has promoted an effort to develop different types of autonomous vehicles that enable the collection of such data. These platforms have varying capabilities of communication, durability, mobility, capacity and autonomy. Within these different platforms, are in addition to others, AUVs and autonomous surface vehicles (ASVs) [10-18, 27].

According to D. Blidber et al. [10], there are three main limitations in autonomous underwater vehicles: energy, navigation over a long period of time and long distances and user communication with the platform. He argued that the use of solar energy begins to overcome these limitations by adding to the submarine's ability to regenerate energy when needed, giving the ability to last for weeks and months on mission, instead of hours. D. Blidber et al. [11] discuss power management in different situations and find an optimum combination of the size needed to store energy and the travel distance measurement and/or works to be undertaken by the vehicle depending on the solar energy available in the area. Special effort is made in the balance between displacement (speed and distance) and tasks (duration and frequency of measurements, number of sensors on board). Their study raises a number of scenarios, where the energy is distributed in different ways, according to the needs of the mission in question, but it is possible to select different settings for each scenario.

The SAUV II vehicle, described in [12-15], is a solar powered AUV designed for long endurance missions such as monitoring, surveillance, or station keeping, with bi-directional communication in real time and underwater instrumentation. The SAUV II operates continuously for several months using solar energy to recharge its lithium ion batteries during daylight hours.

A new long duration solar powered ASV for oceanographic and atmospheric scientific research missions is presented in [16-17]. A fleet of three Ocean Atmosphere Sensor Integration System (OASIS) ASV platforms has been developed under a grant from the National Oceanic and Atmospheric Administration (NOAA) to provide a low-cost, reusable, re-configurable, long-duration, ocean observing capability to support on-going research in key areas, such as carbon dioxide air-sea flux and phytoplankton productivity. The OASIS ASV platform is comprised of five major subsystems. The structural subsystem includes the deck/hull components, mast and internal mounts. The power subsystem contains six 170-watt solar panels, an automated charge controller, twelve 12-volt deep cycle gel cell marine batteries, DC-DC converters, isolators, a power bus and a fuse bank. The propulsion subsystem includes the rudder and propeller control surfaces, as well as the motors, drivers and controllers to operate them. The vehicle computer, communications hardware, navigation sensors, adapters and relay bank are among the components contained in the onboard control subsystem. The payload subsystem includes a suite of standard water and atmospheric sensors.

The AAS Endurance is an autonomous surface vehicle and is detailed by H. Klinck et al. [18] as a project to be developed in three years, driven by the Austrian Society for Innovation in Computer Science, State University of Austria and the Oregon State University. It is an autonomous sailing boat, which uses sensors, actuators and an intelligent control system to manage without being driven. This autonomous marine vehicle has special equipment for the study of marine mammals. It is noteworthy that it has solar panels that generate up to 285W and a methanol fuel cell that supplies auxiliary 65W.

In this paper, an autonomous vehicle capable of operating during long periods of time for observation and monitoring is proposed. The vehicle integrates photovoltaic panels and a methanol fuel cell, together with neurobiologically inspired control architecture for intelligent navigation. In this work, the autonomy of the vehicle is evaluated in several scenarios, when the vehicle is moving in mission and when the vehicle is not moving. The energetic management module generates recharge missions with a variable priority level depending on the batteries' level.

1.3 Autonomous Navigation with Obstacle Avoidance using Neural Networks

Trajectory generation with obstacle avoidance is a fundamentally important issue in robotics. Real-time collision-free trajectory generation becomes more difficult when robots are in a dynamic, unstructured environment. There are a lot of studies on trajectory generation for robots using various approaches to the problem (e.g., [5, 19-23]). Some of the previous models (e.g., [21-22, 24]) use

global methods to search for possible paths in the workspace, which normally deal with static environments only and are computationally expensive when the environment is complex. Seshadri and Ghosh [1] proposed a new path-planning model using an iterative approach. However, this model is computationally complicated, particularly in a complex environment. Li and Bui [2] proposed a fluid model for robot path planning in a static environment. Oriolo et al. [19] proposed a model for real-time map building and navigation for a mobile robot, where a global path planning plus a local graph search algorithm and several cost functions are used.

Several neural network models (e.g., [20-26]) were proposed to generate real-time trajectories through learning. Ritter et al. [22] proposed a Kohonen's self-organizing mapping algorithm based neural network model to learn the transformation from Cartesian workspace to the robot manipulator joint space. Fujii et al. [20] proposed a multilayer reinforcement learning based model for path planning with a complicated collision avoidance algorithm. However, generated trajectories using learning based approaches are not optimal, particularly during the initial learning phase.

However, mathematical models of neuronal systems are a link between biology and engineering. Chang and Gaudiano [29] introduced a neural network for obstacle avoidance that is based on a model of classical and operant conditioning.

In the classical conditioning paradigm, learning occurs by repeated association with a Conditioned Stimulus (CS), which normally has no particular significance for an animal and with an Unconditioned Stimulus (UCS), which has significance for an animal and always gives rise to an Unconditioned Response (UCR). The response that is elicited by the CS after classical conditioning is known as the Conditioned Response (CR) [30-31]. Hence, classical conditioning is the putative learning process that enables animals to recognize informative stimuli in the environment.

In the case of operant conditioning, an animal learns the consequences of its actions. More specifically, the animal learns to exhibit more frequently a behaviour that has led to a reward in the past and to exhibit less frequently a behaviour that led to punishment. In the field of neural networks research, it is often suggested that neural networks based on associative learning laws can model the mechanisms of classical conditioning, while neural networks based on reinforcement learning laws can model the mechanisms of operant conditioning [29, 32]. The reinforcement learning is used to acquire navigation skills for autonomous vehicles and updates both the vehicle model and optimal behaviour at the same time [24, 33-38].

In this paper, the autonomous navigation system of the underwater vehicle consisting of a Self-Organization Direction Mapping Network (SODMN) and a Neural Network for the Avoidance Behaviour (NNAB), both of which are biologically inspired, is presented. The SODMN is a kinematic adaptive neuro-controller and a real-time, unsupervised neural network that learns to control autonomous underwater and surface vehicles in a nonstationary environment. The SODMN combines associative learning and Vector Associative Map (VAM) learning [24, 28, 36-38] to generate transformations between spatial and velocity coordinates. The transformations are learned in an unsupervised training phase, during which the vehicle moves as a result of randomly selected velocities of its actuators. The controller learns the relationship between these velocities and the resulting incremental movements. The NNB is a neural network based on animal behaviour that learns to control avoidance behaviours in autonomous vehicles based on a form of animal learning known as operant conditioning. Learning, which requires no supervision, takes place as the vehicle moves around a cluttered environment with obstacles.

The biologically inspired neural networks proposed in this paper represent a simplified way to understand in part the mechanisms that allow the brain to collect sensory input to control adaptive behaviours in autonomous navigation of animals. In this work, the autonomy of the vehicle is evaluated in several scenarios

This paper is organized as follows. We first describe (Section II) the experimental platform with the navigation system, neural control system and the set of oceanographic instruments installed on the AUV of the Universidad Politécnica de Cartagena (UPCT), called AEGIR. Section III addresses the power management module, which generates recharge missions using the solar panels and fuel cell. The autonomous navigation system of the underwater vehicle is described in Section IV. Section V addresses the experimental results of the proposed control system for controlling avoidance and approach behaviour in the AUV-UPCT. Finally, in Section VI, conclusions based on the experimental results are given.

2. Description of the Solar Powered – Autonomous Underwater Vehicle (SOLAR-AEGIR)

The technical and functional main system requirements of the Solar-AEGIR are:

- Operate autonomously at sea in periods of time from days to weeks.
- Operate at depths up to 50m.
- Operate at speeds up to 4 knots.
- Recharge batteries from photovoltaic panels and methanol fuel cell.

- Continuous communication with a remote operator via a wireless Internet connection.
- Autonomous navigation between two points over a predefined trajectory.
- Capability to capture photos and videos of the underwater environment through a video camera.
- Capability to identify obstacles through imaging sonar.
- Capability to obtain images of the seabed.
- Absolute positioning of the vehicle through GPS and geodetic reference of all data sensors.

Figure 1 shows a 3D drawing of the overall system. The vehicle coordinate system has six velocity components of motion (surge, sway, heave, derivate of roll, derivative of pitch and derivative of yaw). The velocity vector in the vehicle coordinate system is expressed as $\dot{q} = [u\ v\ w\ p\ q\ r]^T$. The global coordinate system OXYZ is a fixed coordinate system. Translational and rotational movement in the global reference frame are represented by $\mathbf{x} = [x\ y\ z\ \varphi\ \theta\ \psi]^T$, which includes earth fixed positions and Euler angles. The surface boat contains a GPRS modem, a GPS receiver, two photovoltaic panels and a methanol fuel cell. The underwater vehicle contains the control and navigation units and the perception systems with sonars, a video camera and a multi-parametric probe. The two vehicles are connected with an underwater cable with Ethernet CAT5e and six 18AWG cables for power, which support up to 500kg of traction.

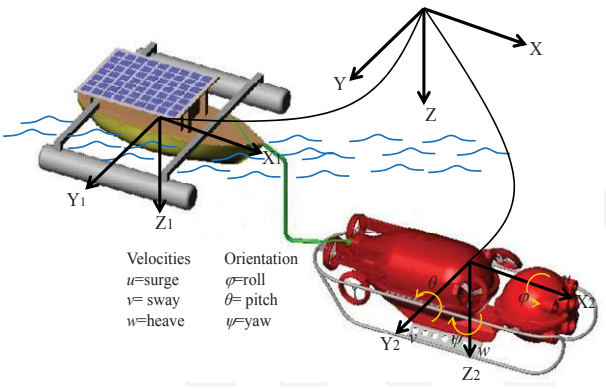

Figure 1. 3D Drawing of Solar-AEGIR. The autonomous vehicle is capable of operating during long periods of time for observation and monitoring.

A block diagram with all the elements integrated in the overall system is shown in Figure 2. The boat has two BP340J multi-crystalline photovoltaic panels, which together generate a maximum power of 80W. These panels have 36 cells in a 4x9 matrix connected in series. The panels are connected to the solar charge regulator SS-MPPT-15L, which features a smart tracking algorithm that maximizes the solar energy harvest from the PV system. The boat includes two $LiFePO_4$ batteries with PCM (protection circuit module). The PCM manages the internal cells and provides overcharge and discharge protection. A methanol fuel cell, EFOY Pro2200, is included to produce energy when the panels do not generate enough energy. This fuel cell has 90W of nominal power and a charging capacity of 2160Wh/day. A GPS receptor for marine application is included in the boat. For communication, the boat integrates an eWON 2005CD, this device establishes a wireless VPN connection with the remote operator station.

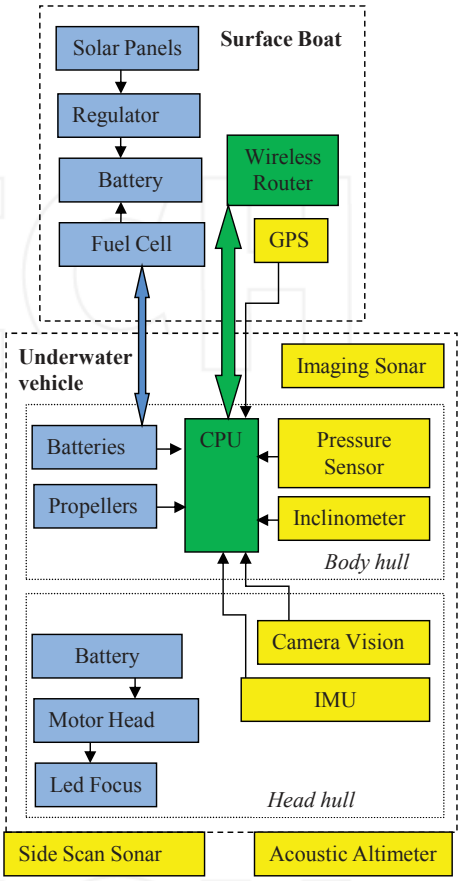

Figure 2. Block diagram of all the elements integrated into the Solar Powered - Autonomous Underwater Vehicle.

The underwater vehicle is waterproof to 300m, although this capability is limited to 50m by the umbilical connection with the surface boat. Its dimensions are 1600 x 600 x 635 mm (LxWxH) and its weight in air is 168kg.

The underwater vehicle has two hulls: the body hull which incorporates the package of batteries, propellers, CPU, an inclinometer and a pressure sensor and the head hull, which includes the perception device (video camera, imaging sonar, side scan sonar, acoustic altimeter and positioning unit). The battery package is composed of eight $LiFePO_4$ batteries with PCM providing 96Ah of capacity. The vehicle has five propellers, two main propellers, two vertical thrusters and one transversal thruster. The hull body incorporates a Crossbow CXTA02 inclinometer, which measures the roll and pitch angles. The pressure sensor is a piezoelectric sensor with a range of up to 300m of depth. The video camera takes photos

and videos; the sight angle can be varied by the head motors. The head hull integrates three 5W led focuses, each one of them with an equivalent halogen power of 35W. The inertial measurement unit (IMU) contains accelerometers, gyroscopes and magnetometers in 3D, with a signal processor, which provides real-time drift-free 3D orientation as well as calibrated 3D acceleration, 3D rate of turn and 3D earth-magnetic field data. The underwater vehicle integrates outside the hulls an acoustic altimeter to provide an accurate height of the seabed. Also, the vehicle incorporates obstacle avoidance sonar characterized by a scan sector up to 360° and a range setting from 2m to 75m. Also, the vehicle includes side-scan sonar for a wide range of seabed survey and inspection duties. Figure 3 shows the SOLAR-AEGIR at Mar Menor lagoon in order to carry out evaluation tests on the navigation system and power management for on-going missions.

(a) (b)

Figure 3. Test of navigation on the Mar Menor lagoon. (a) Underwater Submarine. (b) Surface boat.

3. Power Management of Underwater Vehicle

The energetic system of the vehicle has two circuits, one for control and the other for powering the motors. All of the energetic system works at 24V, although the power circuit can be configured to 48V. The power management module implemented is based on [36]. The power management module takes measurements of the main voltages and currents of the energetic system and makes balances, estimations and predictions about the energy consumption and autonomies of the missions. The energetic system has three operation modes: operation, continuous recharge and deep recharge. In the operation mode the system is recharged only by solar energy and all the elements are in operation. In the continuous recharge mode the system recharges the batteries from the solar panels and the fuel cell and all the elements are in operation. In the deep recharge mode the motors are stopped, the perception system is disconnected and the system recharges from the solar panels and the fuel cell.

The average consumption and energy inputs for the vehicle are shown in Table 1. The energy for the vehicle is shown in Table 2. In Table 3 a summary of the energy balance in operation mode is shown, in this case the vehicle is in operation and only the solar contribution is connected. Table 4 shows the energy data of this mode; in this case the solar panels and the fuel cell are connected. Table 5 shows the deep recharge mode, in this case the motors are stopped and the solar and fuel cells are connected and the batteries are charged.

Elements	Values
Perception Circuit Consumption	1.8 A
Control Circuit Consumption	2,6 A
Power Circuit Consumption	0 A (Motors stopped)
Solar Contribution	2.3 A
Fuel Cell Contribution	3.75 A

Table 1. Consumption and energy inputs.

Elements	Values at 24V
Batteries	120 Ah
Fuel Cell	3.100 Ah

Table 2. Energy in vehicle.

Elements	Values at 24V
Total Consumption	9.4 A
Total Generation	2.3 A
Batteries Contribution	7.1 A
Operating time	5 h

Table 3. Energy balance at operation mode.

Elements	Values at 24V
Total Consumption	9,4 A
Total Generation	6,05 A
Batteries Contribution	3,35 A
Operating time	10,7 h

Table 4. Energy balance at continuous recharge mode.

Elements	Values at 24V
Total Consumption	2.6 A
Total Generation	6.05 A
Batteries Contribution	-3.45 A
Operating Time	unlimited

Table 5. Energy balance at deep recharge mode.

4. Autonomous Navigation System Based on a Biologically Inspired Neural Architecture

The main goal of the navigation system is to achieve an appropriate level of spatial location at all times, allowing trajectory correction using a neural control algorithm to process the corresponding corrections.

A global positioning system (GPS) and a RF communications system on the surface vehicle are mounted for an automatic location. In deep waters, the neural control system represents the most suitable system

for avoiding obstacles and determines the spatial location of the vehicle.

The relative position of the underwater vehicle to the surface vehicle is given by an inertial navigation system combined with the control algorithm and a calibration of positioning bathymetric points of reference. In addition, in case of loss of the expected location, a complementary algorithm is included to allow the vehicle to search and find the seafloor reference.

4.1 Neural Control System

Figure 4 illustrates our proposed neural architecture. The trajectory tracking control without obstacles is implemented by the SODMN and the avoidance behaviour of obstacles is implemented by a neural network of biological behaviour.

For dynamic positioning in path tracking a PID controller was incorporated into the architecture of the control system. It allows the error signal to be smoothed in the reaching of objectives.

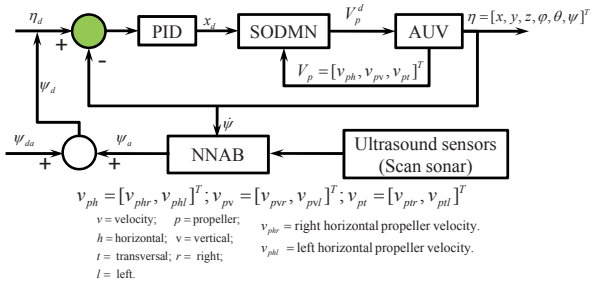

Figure 4. Neural architecture for reactive and adaptive navigation of an AUV.

4.2 Trajectory Tracking Control

The Self-organization Direction Mapping Network (SODMN) learns to control the robot through a sequence of spontaneously generated random movements (shown in Figure 5). The random movements enable the neural network to learn the relationship between angular velocities applied at the propellers and the incremental displacement that ensues during a fixed time step. The proposed SODMN combines associative learning and Vector Associative Map (VAM) learning [28, 36] to generate transformations between spatial coordinates and coordinates of propellers' velocities. The nature of the proposed kinematic adaptive neuro-controller is that it continuously calculates a vectorial difference between the desired and actual velocities, the underwater robot can move to arbitrary distances and angles even though during the initial training phase it has only sampled a small range of displacements.

Furthermore, the online error-correcting properties of the proposed architecture endow the controller with many useful properties, such as the ability to reach targets in spite of drastic changes in the robot's parameters or other perturbations.

At a given set of angular velocities the differential relationship between underwater robot motions in spatial coordinates and angular velocities of propellers is expressed by linear mapping. This mapping varies with the velocities of the propellers.

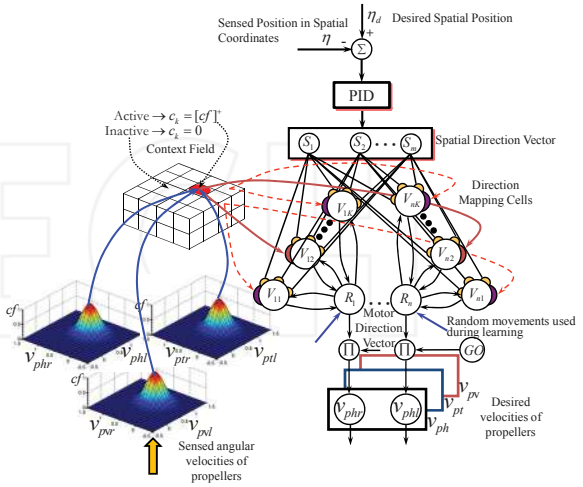

Figure 5. Self-organization direction mapping network (SODMN) for the trajectory tracking of an AUV robot.

The transformation of spatial directions to the propellers' angular velocities is shown in Figure 5. The tracking spatial error (e) is computed to obtain the desired spatial direction vector ($\boldsymbol{x}_d$) and the spatial direction vector (DVs). The DVs is transformed by the direction mapping network elements V_{ik} to corresponding motor direction vector (DVm). On the other hand, a set of tonically active inhibitory cells, which receive broad-based inputs that determine the context of motor action, was implemented as a context field. The context field selects the V_{ik} elements based on the propellers' angular velocities configuration.

A speed-control GO signal acts as a nonspecific multiplicative gate and controls the movement's overall speed. The GO signal is an input from a decision centre in the brain and starts at zero before movement and then grows smoothly to a positive value as the movement develops. During learning, the sensed angular velocities of propellers are fed into the DVm and the GO signal is inactive.

The activities of cells of the DVs are represented in the neural network by quantities (S_1, S_2, ⋯, S_m), while the activities of the cells of the motor direction vector (DVm) are represented by quantities (R_1, R_2, ⋯, R_n). The direction mapping is formed with a field of cells with activities V_{ik}. Each V_{ik} cell receives the complete set of spatial inputs S_j, $j = 1, \ldots, m$, but connects to only one R_i cell (see Figure 5). The mechanism that is used to ensure weights converge

to the correct linear mapping is similar to the VAM learning construction [28]. The direction mapping cells ($\mathbf{V}\in\mathbf{R}^{n\times k}$) compute a difference in activity between the spatial and motor direction vectors via feedback from the DVm. During learning, this difference drives the adjustment of the weights. During performance, the difference drives DVm activity to the value encoded in the learned mapping.

A context field cell pauses when it recognizes a particular velocity state (i.e., a velocity configuration) in its inputs and thereby disinhibits its target cells. The target cells (direction mapping cells) are completely shut off when their context cells are inactive. This is shown in Figure 5. Each context field cell projects to a set of direction mapping cells, one for each velocity vector component. Each velocity vector component has a set of direction mapping cells associated with it, one for each context. A cell is "*on*" for a compact region of the velocity space. It is assumed for simplicity that only one context field cell turns "*on*" at a time. In Figure 5, inactive cells in the context field are shown as white disks. The centre context field cell is "*on*" when the angular velocities are in the centre region of the velocity space, in this three degree-of-freedom example. The "*on*" context cell enables a subset of direction mapping cells through the inhibition variable ck, while the "*off*" context cells disable the other subsets. When the k^{th} context cell is "*off*" or inactive (modelled as c_k=0) in its target cells, the entire input current to the soma is shunted away such that there remains only activity in the axon hillock, which decays to zero. When the k^{th} context cell is "*on*" or active, c_k =1, its target cells (V_{ik}) receive normal input.

Learning is obtained by decreasing weights in proportion to the product of the presynaptic and postsynaptic activities [22, 24, 28, 36]. Therefore, the learning rule can be obtained by using the gradient-descent algorithm. The training is done by generating random movements and by using the resulting angular velocities and observed spatial velocities of the AUV robot as training vectors to the direction-mapping network.

4.3 Obstacle Avoidance Adaptive Neuro-Controller

The obstacle avoidance adaptive neuro-controller is a neural network that learns to control avoidance behaviours in an AUV robot based on a form of animal learning known as operant conditioning. Learning, which requires no supervision, takes place as the robot moves around a cluttered environment with obstacles. The neural network for avoidance behaviours (NNAB) requires no knowledge of the geometry of the robot or of the quality, number, or configuration of the robot's sensors (shown in Figure 6). Our implementation is based on the Grossberg's conditioning circuit, which follows closely that of Grossberg & Levine [30, 31] and Chang & Gaudiano [29].

In this model the sensory cues (both conditioned stimuli (CS) and unconditioned stimuli (UCS)) are stored in Short Term Memory (STM) within the population labelled S_T, which includes competitive interactions, to ensure that the most salient cues are contrast enhanced and stored in the STM while less salient cues are suppressed.

The population S_T is modelled as a recurrent competitive field in a simplified discrete-time version, which removes the inherent noise and efficiently normalizes and contrast-enhances the ultrasound sensors activations. In the present model the CS nodes correspond to activation from the robot's sonar sensors. In the network, I_i represents a sensor value, which codes proximal objects with large values and distal objects with small values. The drive node (D) corresponds to the Reward/Punishment component of operant conditioning (an animal/robot learns the consequences of its own actions).

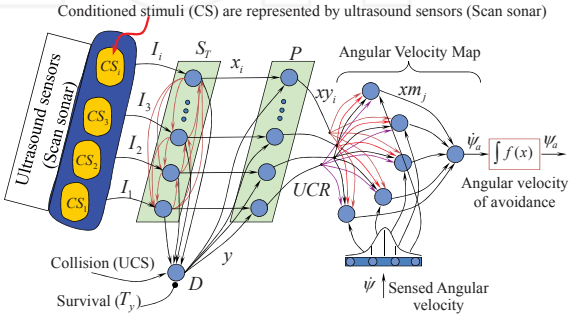

Figure 6. Neural network for the avoidance behaviour (NNAB).

Learning can only occur when the drive node is active. Activation of the drive node (D) is determined by the weighted sum of all the CS inputs, plus the UCS input, which is presumed to have a large, fixed connection strength, plus a homeostatic signal corresponding to a sort of "survival instinct" (T_y), which is active at all times and is a threshold that controls how easily the drive node is activated. The drive node is active when the robot collides with an obstacle, which could be detected through a collision sensor, or when any one of the sonar sensors indicates that an obstacle is closer than the sensor's minimum range. Then the unconditioned stimulus (USC) in this case corresponds to a collision detected by the robot. The activation of the drive node and of the sensory nodes converges upon the population of polyvalent cells (P). Polyvalent cells require the convergence of two types of inputs in order to become active. In particular each polyvalent cell receives input from only one sensory node and all polyvalent cells also receive input from the drive node (D).

Finally, the neurons (xm_j) represent the response (conditioned or unconditioned) and are thus connected to the motor system. The motor population consists of nodes (i.e., neurons) encoding the desired angular velocities of

avoidance, i.e., the activity of a given node corresponds to a particular desired angular velocity for the AUV robot. When driving the robot, activation is distributed as a Gaussian centred on the desired angular velocity of avoidance. The use of a Gaussian leads to smooth transitions in angular velocity, even with few nodes.

The output of the angular velocity population is decomposed by SODMN into the angular velocities of the left and right horizontal thrusters. A gain term can be used to specify the maximum possible velocity. In NNAB the proximity sensors initially do not propagate activity to the motor population because the initial weights are small or zero.

The robot is trained by allowing it to make random movements in a cluttered environment. Specifically, we systematically activate each node in the angular velocity map for a short time, causing the robot to cover a certain distance and rotate through a certain angle depending on which node is activated. Whenever, the robot collides with an obstacle during one of these movements, or comes very close to it, the nodes corresponding to the largest (closest) proximity sensor measurements just prior to the collision will be active.

Before a collision occurs and before any learning has taken place, the CS node sends activation to its corresponding polyvalent cells. However, the connection from the CS node to the drive node is very weak, so that the drive node does not activate. Hence the polyvalent cell only receives one kind of input and it does not become active.

When the same CS node is on at the time of a collision, the UCS causes the drive node to become active. The drive node sends its activation to all polyvalent cells; however, only the polyvalent cell corresponding to the active CS turns on, because it is the only one receiving both kinds of input. At this point, the activation of the drive node allows two kinds of learning to take place simultaneously: the learning that couples sensory nodes (sonar sensors) with the drive node (the collision) and the learning that inhibits the movements of the angular velocity pattern that existed just before the collision.

The first type of learning follows an associative learning law with decay. This learning enables the most active sensory nodes to accrue strength in their connections to the drive node, so that eventually the sensory nodes will be able to activate the drive signal on their own and thus to activate the polyvalent cells (*P*) and ultimately a motor response. The primary purpose of this learning scheme is to ensure that learning occurs only for those CS nodes that were active within some time window prior to the collision (UCS).

The second type of learning, which is also of an associative type but inhibitory in nature, is used to map the sensor activations on the angular velocity map. This learning takes place between the polyvalent cells and the cells that actually generate the robot´s movements, whereby simultaneous activation of the pre- and post-synaptic cells leads to an increasingly large negative (i.e., inhibitory) weight. By using an inhibitory learning law, the polyvalent cells corresponding to the active sensory nodes acquire negative connection weights that learn to generate a pattern of inhibition matching the angular velocity profile active at the time of collision.

Once learning has occurred, the activation of the angular velocity map is given by two components (see Figure 7). An excitatory component, which is generated directly by the sensory system, reflects the angular velocity required to reach a given target in the absence of obstacles. For simplicity here we assume that the angular velocity is proportional to the angle between the robot's current heading and the target. A second, inhibitory component, generated by the conditioning model in response to sensed obstacles, moves the robot away from the obstacles as a result of the activation of sensory signals in the conditioning circuit.

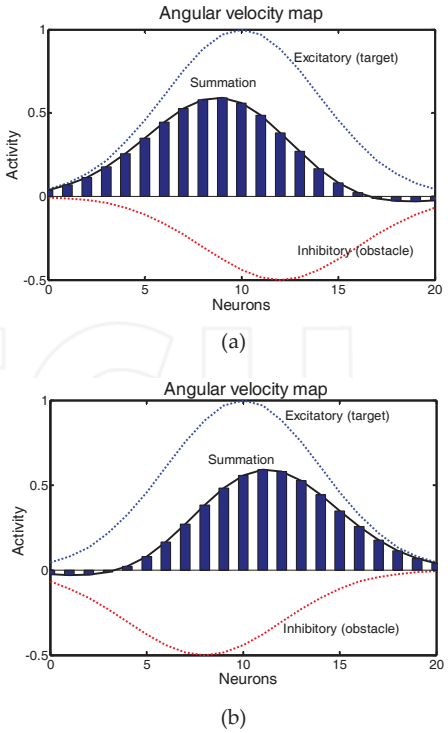

Figure 7. Positive Gaussian distribution represents the angular velocity without obstacle and negative distribution represents activation from the conditioning circuit. The summation represents the angular velocity that will be used to drive the robot. Notice how the maximum peak of the excitatory Gaussian is shifted by the inhibitory Gaussian.

When an excitatory Gaussian is combined with an inhibitory Gaussian at a slightly shifted position, the

resulting net pattern of activity exhibits a maximum peak that is shifted from the excitatory Gaussian in a direction away from the peak of the inhibitory Gaussian. In Figure 7, we superimpose a positive Gaussian centred over the middle of the map and a negative Gaussian to the right. The net pattern of activation shows a positive peak that is shifted to the left of centre. Imagine now that the positive Gaussian represents the angular velocity at which the robot must move to reach a target (straight ahead) and that the negative Gaussian represents an obstacle to the right of the robot. In this case, the two Gaussians interact, causing the robot to turn to the left, avoiding the obstacle. Hence, the presence of an obstacle to the right causes the robot to shift to the left and vice-versa (see Figure 7b).

5. Experimental Results

High-level control algorithms (SODMN and NNAB) are written in VC++ and run with a sampling time of 10ms on an embedded CPU (Matrix MXC-6101-D) with an Intel core i7™ 620LE to 2.0 GHz and chipset QM57. The lower level control layer is in charge of the execution of the high-level velocity commands. It consists of a distributed control system based on CANOPEN nodes with a master based on NI CRIO.

The first tests of navigation on the surface and immersion were performed in a pool. The robot was immersed in a 15m deep controlled pool in the industrial area of Fuente Álamo, Murcia-Spain. These tests confirmed the manoeuvrability of the vehicle and the response sensitivity of the controls in remote mode. Navigation tests verified directional stability, turns and immersions. In all cases we were able to verify the correct response to requests from the vehicle operator. The test was developed for about an hour, at which time the battery charge did not show signs of exhaustion and for a period of 120 hours where the solar panels and fuel cell worked to keep the batteries charged. It could also verify the accuracy of the measurement of the total displacement of the submerged vehicle, a fact that is essential to being able to properly ballast in each future operation.

Importantly, the AUV must be trained in remotely operated vehicle (ROV) mode so that the algorithm learns the manoeuvres of avoidance behaviour and recovery of the path in unexpected situations, in order to implement the procedures in autonomous navigation mode (unmanned AUV). In this first test we have been able to verify the feasibility of the control system. Figure 8 shows the early stages of the navigation tests.

The proposed neural network model is capable of generating an optimal trajectory for underwater vehicles in an arbitrarily varying environment. The state space is the Cartesian workspace of the underwater robot. Figure 9 shows the performance of a trajectory-tracking controller implemented like a SODMN. These tests were carried out in Fuente Alamo-swimming pool in a 3D workspace without any obstacles, with an initial position (P_0) at (x, y, z) = (1, 1, 1)m and an initial orientation as shown in figures as (φ_0, θ_0, ψ_0). Note that the depth was recorded as positive (Z). The approach behaviours and the tracking of a trajectory by the AUV robot with respect to the reference trajectory are shown in Figure 9. The desired trajectory is a sine wave with an initial position of P_{d0} (2, 3, 5)m and a final position of (20, 6, 4)m.

(a)

(b)

Figure 8. Navigation trials at the Mar Menor Lagoon. (a) Surface navigation and successful underwater operation tests. (b) AUV powered by solar energies and fuel cell, operating during long periods of time in order to carry out observation and monitoring.

In our model of NNAB, the range sensors initially do not propagate activity to the motor population because the initial weights are small or zero. The robot is trained by allowing it to make random movements in a cluttered environment. The goal of the training phase is to give each CS node the opportunity to sample several movements that lead to collisions.

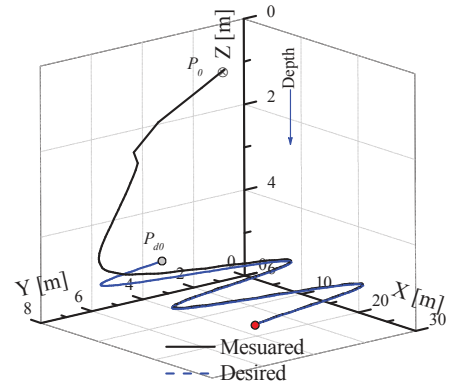

(a)

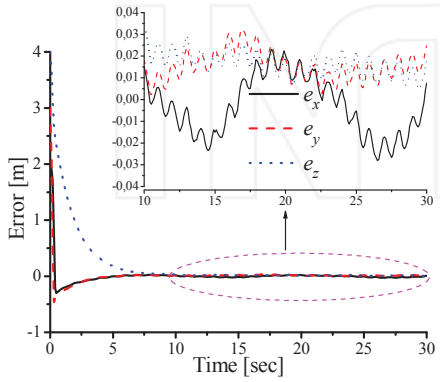

(b)

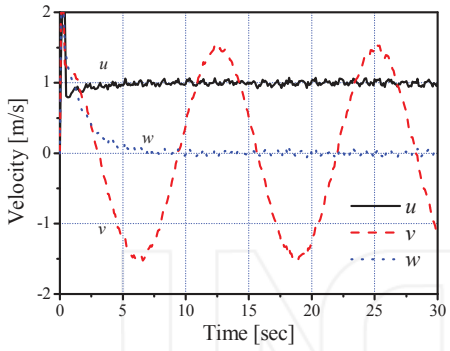

(c)

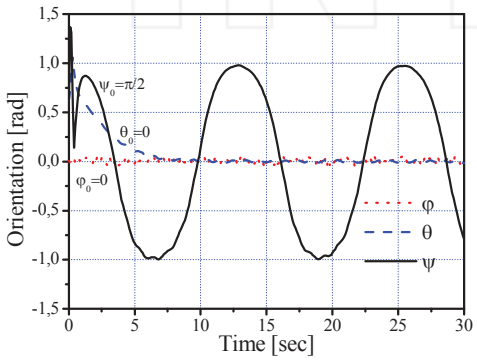

(d)

Figure 9. Tracking control of a desired trajectory. (a) The tracking performance of the AUV. (b) Tracking error. (c) Tracking velocity. (d) Tracking orientation.

In practice we found that it is sufficient for each CS node to be active during only a handful of collisions, when using nodes in the angular velocity map. In order to generate a wide range of movements, during the training phase we turn on each node in the angular map for a brief time until a collision is registered, then switch to a new angular map node and repeat the process. We can achieve good avoidance behaviour in this way with only a few collisions for each node. Figure 10(a) illustrates the learning process. We obtained this curve in the following way: starting with all the weights in the network set to zero, we turn on one node in the angular map and let the robot collide with an obstacle, generating a small amount of learning, then turn on another node and so on. At regular intervals during the training phase we temporarily disable learning and allow the robot to move from a new starting position for a total of 500 steps through the algorithm and measure in how many of the 500 steps the robot detected a collision. On the first trial, before any learning has taken place, as soon as the robot collides it remains stuck against the obstacle, so the number of collisions is very close to 500. By the time we have trained through 50 collisions (total: meaning that each of the sensory nodes, on average, has sampled fewer than ten collisions. The signal of the avoidance sonar is discomposed in ten sensory nodes) the robot is able to navigate with virtually no collisions.

The inhibitory weights developed by the neural network are depicted in Figure 10(b). The adaptive connections between the sensory nodes and the angular velocity map develop in such a way that angular velocities that make the robot turn to the right (nodes close to 20) are inhibited when the sensors located at the right side of the robot are active (sensory nodes 6 and 10). Similar yet opposite inhibitory weights develop for left turns when obstacles are sensed at the left side. In the middle of the figure (nearly straight-forward movements with obstacles located straight ahead), a Gaussian-like inhibitory curve accounts for the fact that in such cases turns to either the left or the right are needed to avoid collisions.

To carry out these tests of obstacle avoidance the Mar Menor coastal Lagoon was chosen. The Mar Menor is a hyper saline coastal lagoon located in the Region of Murcia (Spain) in the South Western Mediterranean Sea. Its special ecological and natural characteristics make the lagoon a unique natural water body, being the largest lagoon in Europe. Its General characteristics are: 6-10m max. depth, 135km^2 area, 2.5m mean depth and 42-49 P.S.U. salinity. Figure 11 shows the Mar Menor Lagoon.

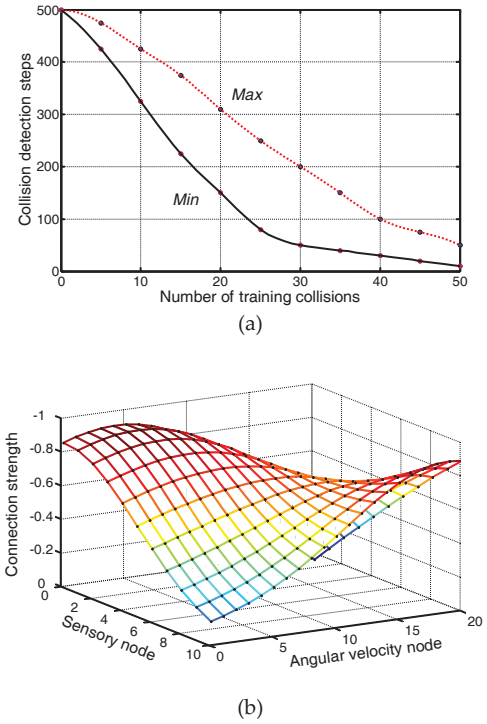

Figure 10. Results of the learning process of NNAB. (a) Learning in the AUV, measured as the number of collisions in steps as a function of the total number of collisions experienced during training. Min and Max refer to the best and worst learning curves out of a set of five training trials. (b) Adaptive connections between the sensory nodes and the angular velocity map developed by the AUV for the obstacle avoidance behaviour.

Figure 11. Location of the study zone. Aerial view of the Mar Menor lagoon, in Murcia, Spain.

Figure 12 shows the NNAB's performance with the presence of several obstacles. The underwater robot starts from the initial position P_0=(10,30,1)m and reaches a desired position (goal). During the movements, whenever the underwater robot is approaching an obstacle (boat), the inhibitory profile from the conditioning circuit (NNAB) changes the selected angular velocity and makes the underwater robot turn away from the obstacle. The presence of multiple obstacles at different positions in the underwater robot's sensory field causes a complex pattern of activation that steers the underwater robot between obstacles.

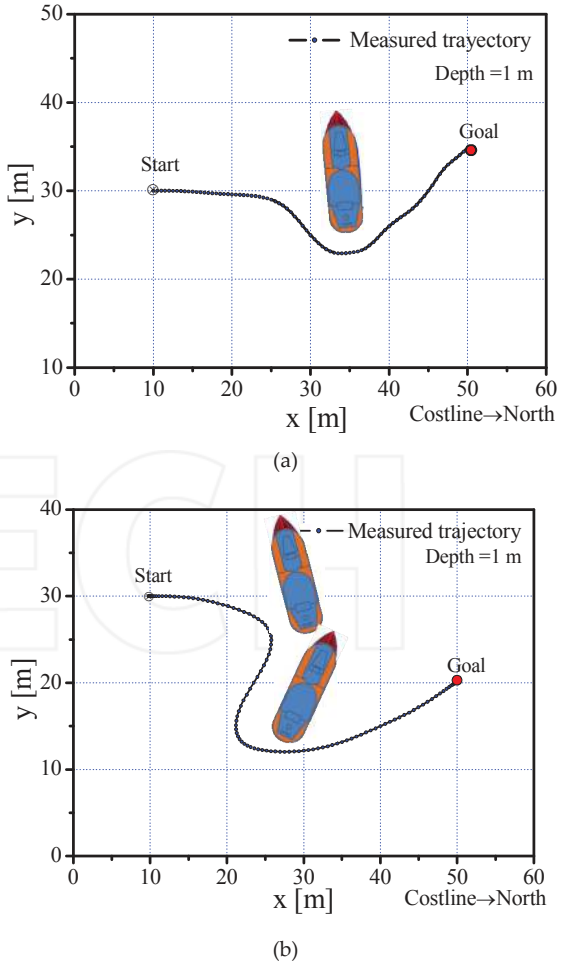

Figure 12. Obstacle avoidance trajectory with a goal of (50,35,1)m in (a) and of (50,20,1)m in (b).

6. Conclusion

The aim of this work was to design a Solar Unmanned Underwater Vehicle for long-term operations, for which two aspects were particularly important: energy and navigation. The energetic aspect is addressed by including photovoltaic panels, a fuel cell and a module manager to monitor the power status of the vehicle and the navigation aspect is addressed by creating a multi-sensory architecture and multi-network on the basis of cortical areas involved in motion planning, trajectory and the task. In this article, we have implemented a neurobiologically inspired neural architecture for the navigation system of a solar powered Unmanned Underwater Vehicle. This neural architecture allows trajectory tracking and obstacle avoidance behaviours online in unstructured and unknown environments. A biologically inspired neural network for spatial reaching tracking has been developed. This neural network is implemented as a kinematical adaptive neuro-controller. The avoidance behaviours of obstacles were implemented by a neural network that is based on a form of animal learning known as operant conditioning.

The efficacy of the proposed neural architecture has been successfully demonstrated in experimental results for the trajectory tracking and reaching, as well as avoidance behaviours of the underwater robot. Tests carried out confirm the validity of the platform for its use as a multitasking vehicle for oceanographic research and missions. Due to the ability to carry out operations under remote control and when autonomous, the AUV-UPCT is suitable for a wide variety of missions foreseen for the future.

7. Acknowledgement

Authors thank the Spanish Navy for its support in the development of the unmanned underwater vehicle from UPCT for environmental and oceanographic studies. This project is in part supported by the Coastal Monitoring System for the Mar Menor (CMS- 463.01.08_CLUSTER) project founded by the Regional Government of Murcia, by the SICUVA project (Control and Navigation System for AUV Oceanographic Monitoring Missions. REF: 15357/PI/10) founded by the Seneca Foundation of Regional Government of Murcia and by the DIVISAMOS project (Design of an Autonomous Underwater Vehicle for Inspections and oceanographic mission-UPCT: DPI-2009-14744-C03-02) founded by the Spanish Ministry of Science and Innovation from Spain.

8. References

[1] C. Seshadri and A. Ghosh, Optimum path planning for robot manipulators amid static and dynamic obstacles, *IEEE Trans. Syst. Man and Cybern.,* vol. 23, 1993, pp. 576-584.

[2] Z.X. Li and T.D. Bui, Robot path planning using fluid model, *J. Intell. Robot. Syst., vol. 21*, 1998, pp. 29-50.

[3] D.R. Yoerger and J.E. Slotine, Robust trajectory control of underwater vehicles, *IEEE J. Ocean Eng.*, vol. 10, issue: 4, October 1985, pp. 462-476.

[4] Y. Nakamura and S. Savant, Nonlinear tracking control of autonomous underwater vehicles. *Proceeding IEEE International Conference on Robotics and Automation*, May 1992, pp. A4-A9, Nice, France.

[5] G. Antonelli, S. Chiaverini, N. Sarkar and M. West, Adaptive control of an autonomous underwater vehicle: experimental results on ODIN, *IEEE Trans Control Syst. Technol.*, vol. 9, issue: 5, Sep. 2001, pp. 756-765.

[6] J. Lorentz and J. Yuh, A survey and experimental study of neural network AUV control, *Proceedings of the 1996 Symposium on Autonomous Underwater Vehicle Technology-IEEE AUV'96*, June 2-6, 1996, pp. 109-116, Monterey, CA, USA.

[7] V.W. Porto and D.B. Fogel, Neural network for AUV guidance control, *Sea Technology,* vol. 33, issue: 2, February 1992, pp. 25-35.

[8] S.M. Smith, G.J.S. Rae and D.T. Anderson, Applications of fuzzy logic to the control of an autonomous underwater vehicle. *Second IEEE International Conference on Fuzzy Systems*, vol. 2, March 28-April 01, 1993, p. 1099–1106, San Francisco, CA, USA.

[9] C. Silpa-Anan, T. Brinsmead, S. Abdallah and A. Zelinsky, Preliminary experiments in visual servo control for autonomous underwater vehicle, In *Proceedings of IEEE/RSJ International Conference on Intelligent Robotics and Systems* (IROS'2001), vol. 4, October 29-November 03, 2001, pp.1824-1829, Maui, HI, USA.

[10] D.R. Blidberg, J.C. Jalbert and M.D. Ageev, Experimental results: The AUSI/IMTP solar powered AUV project, *Interservice/Industry, Training, Simulation, and Education Conference*, Dec. 4-7, 2006, Orlando, Fl, U.S.A.

[11] D.R. Blidberg, M.D. Ageev and J. Jalbert, Some design considerations for a solar powered AUV; Energy management and its impact on operational characteristics, *Proceedings of the 10th International Symposium on Unmanned Untethered Submersible Technology*, September 5-11, 1997, Autonomous Undersea Systems Institute, Durham, NH, USA.

[12] D.M. Crimmins, C.T. Patty, M.A. Beliard, J. Baker, J.C. Jalbert, R.J. Komerska, S.G. Chappell and D.R. Blidberg, Long-Endurance Test Results of the Solar-Powered AUV System, *Proceedings of IEEE/MTS OCEANS 2006 Conference*, September 18-21, 2006, Boston, MA, USA.

[13] D. Crimmins, E.K. Hinchey, M.C. Chintala, G. Cicchetti, C. Deacutis and D.R. Blidberg, Use of a long endurance solar powered autonomous underwater vehicle (SAUV II) to measure dissolved oxygen concentrations in Greenwich Bay, Rhode Island, U.S.A., *Proceeding of IEEE, Oceans 2005 – Europe*, vol. 2, 2005, pp. 896 – 901, Piscataway, NJ, USA.

[14] T.B. Curtin, D. M. Crimmins, J. Curcio, M. Benjamin and C. Roper, Autonomous Underwater Vehicles: Trends and Transformations, *Marine Technology Society Journal,* vol. 39, Issue: 3, 2005, pp. 65-75.

[15] S.G. Chappell, S.S. Mupparapu, R.J. Komerska and D.R. Blidberg, SAUV II High Level Software Architecture, *Proceedings of the Fourteenth International Symposium on Unmanned Untethered Submersible Technology*, Autonomous Undersea Systems Institute, August, 2005, Lee, NH, USA.

[16] J. Higinbotham, J. Moisan and P. Hitchener, Development of a New Long Duration Solar Powered Autonomous Surface Vehicle, *Proceedings of IEEE/MTS OCEANS 2006 Conference*, September 18-21, 2006, Boston, MA, USA.

[17] J.R. Higinbotham, J.R. Moisan, C. Schirtzinger, M. Linkswiler, J. Yungel and P. Orton, Update on the

development and testing of a new long duration solar powered autonomous surface vehicle, *Proceedings of IEEE, Oceans 2008*, September 15-18, 2008, pp. 1-10, Quebec City, QC, Canada.

[18] H. Klinck, K. Stelzer, K. Jafarmadar and D. K. Mellinger, AAS Endurance: An Autonomous acoustic sailboat for marine mammal research, *Proceedings of the robotic sailing conference (IRCS)*, July 2009, pp. 43-48, 2009, Matosinhos, Portugal.

[19] G. Oriolo, A. D. Luca and M. Vendittelli, WMR control via dynamic feedback linearization: Design, implementation and experimental validation, *IEEE Trans. Control. Syst. Technol*., vol. 10, 2002, pp. 835-852.

[20] T. Fujii, Y. Arai, H. Asama and I. Endo, Multilayered reinforcement learning for complicated collision avoidance problems. *Proceedings IEEE International Conference on Robotics and Automation*, vol. 3, 1998, pp. 2186-2191, Leuven, Belgium.

[21] M. Carreras, J. Yuh, J. Batlle and P. Ridao, A behavior-based scheme using reinforcement learning for autonomous underwater vehicles, *IEEE Journal of Oceanic Engineering*, vol. 30, Issue: 2, 2005, pp. 416-427.

[22] H.J. Ritter, T.M. Martinez and K.J. Schulten, Topology-conserving maps for learning visuo-motor coordination, *Neural Networks,* vol. 2, 1989, pp. 159-168.

[23] F. García-Córdova, A cortical network for control of voluntary movements in a robot finger, *Neurocomputing*, vol. 71, 2007, pp. 374-391.

[24] F. García-Córdova, A. Guerrero-González and F. Marín-García, Design and implementation of an adaptive neuro-controller for trajectory tracking of nonholonomic wheeled mobile robots, In Mira, J., Álvarez, J.R., (eds.), *Nature Inspired Problem-Solving Methods in Knowledge Engineering*, Lectures Notes in Computer Science, vol. 4528, Springer-Verlag Berlin Heidelberg, LNCS- 4528, Part II, ISBN: 978-3-540-73054-5, 2007, pp. 459-468.

[25] T. Hacib, M.R. Mekideche, N. Ferkha, Application of RBF neural network and finite element analysis to solve the inverse problem of defect identification, *International Review of Electrical Engineering*, vol. 2, Jan-Feb, 2007, pp. 110-117.

[26] Z. H. Ashour, S. R. Hashem, H.A. Fayed, A new approach for combining neural networks during training for time series modeling, *International Review of Electrical Engieneering*, vol. 2, Issue: 5, Sep-Oct, 2007, pp. 745-750.

[27] C. Benbouchama, M. Tadjine, A. Bouridane, A High-Level Environment for FPGA Neural Network Implementation, *International Review of Electrical Engineering, Part A,* vol. 4, Issue: 6, Nov-Dec, 2009, pp. 1243-1247.

[28] P. Gaudiano and S. Grossberg, Vector associative maps: Unsupervised real-time error-based learning and control of movement trajectories. *Neural Networks*, vol. 4, 1991, pp. 147–183.

[29] C. Chang and P. Gaudiano, Application of biological learning theories to mobile robot avoidance and approach behaviors. *J. Complex Systems*, vol. 1, 1998, pp. 79–114.

[30] S. Grossberg and D. Levine, Neural dynamics of attentionally moduled Pavlovian conditioning: Blocking, interstimulus interval and secondary reinforcement, *Applied Optics*, vol. 26, 1987, pp. 5015–5030.

[31] S. Grossberg, On the dynamics of operant conditioning, *Journal of Theoretical Biology,* vol. 33, 1971, pp. 225—255.

[32] R.S. Sutton and A.G. Barto, Toward a modern theory of adaptive networks: Expectation and prediction, *Psychological Review,* vol. 88, 1981, pp. 135—170.

[33] C. Galindo, J.A. Fernández-Madrigal and J. González, Towards the automatic learning of reflex modulation for mobile robot navigation, *Nature Inspired Problem-Solving Methods in Knowledge Engineering*, J. Mira and J.R. Alvarez (Eds.), IWINAC 2007, Part II. LNCS vol. 4528, 2007, pp. 347-356. Springer, Heidelberg.

[34] C. Galindo, J. González and J.A. Fernández-Madrigal, A control architecture for human-robot integration: Application to robotic wheelchair, *IEEE Trans. On Systems, Man and Cyb. – Part B*, vol. 36, 2006, pp. 1053-1068.

[35] F. Lamiraux and J.P. Laumond, Smooth motion planning for car-like vehicles, *IEEE Trans. Robot. Automat.,* vol. 17, Issue: 4, 2001, pp. 498-502.

[36] A. Guerrero-González, F. García-Córdova and F. de Asis Ruz-Vila, A Solar Powered Autonomous Mobile Vehicle for Monitoring and Surveillance Missions of Long Duration, *International Review of Electrical Engineering,* Part A, vol. 5, Issue: 4, August 2010, pp. 1580-1587.

[37] L. Sorbi, G.P. De Capua, J-G Fontaine and L. Toni, A Behavior-Based Mission Planner for Cooperative Autonomous Underwater Vehicles, Marine Technology Society Journal, vol. 46, Issue: 2, March/April 2012 , pp. 32-44(13).

[38] A. J. Ijspeert, Central pattern generators for locomotion control in animals and robots: A review. *Neural Networks*, vol. 21 Issue: 4, May, 2008, pp. 642-653.